Quantum Information and Computation, Vol. 17, No. 1&2 (2017) 0117–0124

ELECTRICAL CONTROL OF STRONG SPIN-PHONON COUPLING IN A CARBON NANOTUBE

FANG-YU HONG
Department of Physics, Center for Optoelectronics Materials and Devices Zhejiang Sci-Tech University, Hangzhou, Zhejiang 310018, China

JING-LI FU
Department of Physics, Center for Optoelectronics Materials and Devices Zhejiang Sci-Tech University, Hangzhou, Zhejiang 310018, China

YAN WU
Department of Physics, Center for Optoelectronics Materials and Devices Zhejiang Sci-Tech University, Hangzhou, Zhejiang 310018, China

ZHI-YAN ZHU
Department of Physics, Center for Optoelectronics Materials and Devices Zhejiang Sci-Tech University, Hangzhou, Zhejiang 310018, China

Received September 23, 2015
Revised December 26, 2016

We describe an approach to electrically control the strong interaction between a single electron spin and the vibrational motion of a suspended carbon nanotube resonator. The strength of the deflection-induced spin-phonon coupling is dependent on the wavefunction of the electron confined in a lateral carbon nanotube quantum dot. An electrical field along the nanotube shifts the effective center of the quantum dot, leading to the corresponding modification of the spin-phonon strength. Numerical simulations with experimentally reachable parameters show that high fidelity quantum state transfer between mechanical and spin qubits driven by electrical pulses is feasible. Our results form the basis for the fully electrical control of the coherent interconvertion between light and spin qubits and for manufacturing electrically driven quantum information processing systems.

Keywords:

Communicated by: S Braunstein & G Milburn

1 Introduction

Nanomechanical devices have attracted broad interest as they hold promise to find potential applications in fundamental tests of quantum behavior of macroscopic objects, ultrasensitive detection, and quantum information processing [1]. The exceptional mechanical properties of carbon nanotubes (CNTs), their large Young modulus, and low masses on the order of the attogram, make them to be the most conspicuous among all kind of available nanomechanical systems, because these properties result in high resonance frequency and large zero-point motion, which make it possible to greatly enhance the quantum operation speed and to

relieve the demanding experimental conditions for ground-state cooling and state readout.

Moreover, carbon-based systems have many fascinating features for quantum information processing. In a variety of systems like GaAs, the hyperfine interplay between electron and nuclear spins contributes the leading source of electron spin decoherence, which heavily hinders the qubit performance of the single electron spins in a quantum dot defined in these systems. In contrast, we can grow carbon-based systems with pure ^{12}C which is free of net nuclear spin, to completely remove the hyperfine-interaction induced decoherence. Moreover, compared with phonon continuum in bulk materials which imposes main restrictions on the improvement of the electron spin coherence time, the phonon spectrum of a suspended CNT is discretized and can be designed to have a a remarkably low density of states, enabling very long spin lifetimes when the spin energy splitting is off-resonance with the phonon modes. At the same time we can obtain strong spin-phonon coupling for quantum information processing such as qubit rotation, quantum state transfer, or generating entangled states [3, 2], by prompting the spin splitting resonant with a high-Q discrete phonon mode, which can be accomplished by exerting appropriate magnetic field on the spin.

Quantum control of the state of an electron spin is generally accomplished by a resonant oscillating magnetic field. However, it has been proven to be challenging to generate strong oscillating magnetic field in a semiconductor device by specially designed microwave cavities [4] or microfabricated striplines [5]. In contrast, it is far easier to produce electric field by simply exciting a local gate electrode. Furthermore, electric field provides much higher spatial selectivity, which is essential for local individual spin manipulation. Electrical control of a spin-based system for quantum information processing [6, 7] is thus highly desirable. Recently literature [8] theoretically shows that electric spin control and coupling is viable with bends in CNTs. The deflection in a CNT can also lead to strong coupling between an electron spin in a quantum dot and the vibrational motion of the CNT [9, 10]. However the suggested spin-phonon coupling is difficult to modulate when the setup has been shaped up.

Here we propose a scheme for electrical control of the spin-phonon coupling in CNTs. The deflection due to the vibration motion of a suspended CNT couples the CNT vibration motion to an electron spin confined in a lateral CNT quantum dot (QD). The spin-phonon coupling is dependent on the electron density distribution in the QD. An electrical field along the nanotube shifts the effective center of the QD, thus modifies the density distribution, leading to the corresponding electrical control of the spin-phonon strength. Note that when the spin is required to be isolated from the environment the spin-phonon coupling can be easily turned off through the electric field, eliminating the phonon mechanism of decoherence. Numerical simulations show that the high fidelity quantum state transfer between mechanical and spin qubits driven by electrical pulses is within the reach of current technique. Recent experimental advance in fabrication of lateral CNT QD provides the basis for the physical implementation of our proposal [11, 12, 13]. Our results provide the basis for the electrical control of light-spin quantum interface and for manufacturing electrically driven quantum information processing systems.

2 Theoretical model and numerical evaluation

In the setup shown in Fig.1 the suspended CNT confines an electron with a lateral quantum dot. Here we consider most experimentally relevant regime $\Delta_g \gg E_L \gg E_B, E_{SO}, E_{KK'}$,

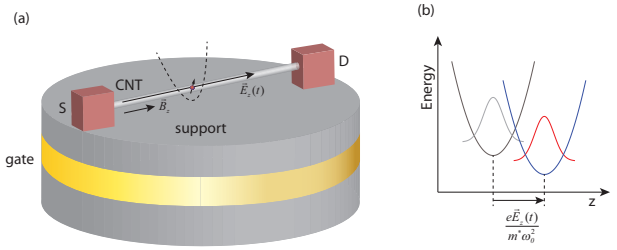

Fig. 1. (color online) (a) Schematic of a lateral quantum dot confining an electron spin on a suspended carbon nanotube. (b) A parallel-to-CNT electric field displaces the effective center of the parabolic potential along the electric field direction and changes the potential depth, ω_0 is the oscillator frequencies of the parabolic quantum dot, and m^* is the effective electron mass. see text for details.

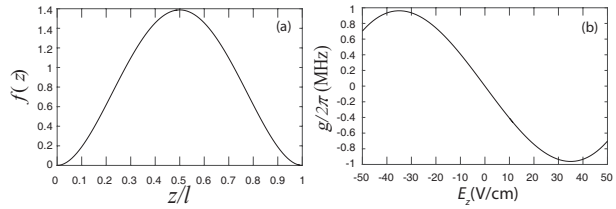

Fig. 2. (a) The dimensionless waveform $f(z)$ of the phonon mode under consideration with normalization $\int_0^l f^2(z)dz = l$. (b) The spin-phonon coupling g versus the electric field E_z. See text for details.

where $2\Delta_g$ is the energy gap between the valence band and the conduction band, E_L is the energy level difference arising from the longitudinal confining potential of the quantum dot $V(z)$, and E_B, E_{SO}, and $E_{KK'}$ are the energy changes caused by the external magnetic field, the spin-orbit coupling, and the intervalley interplay, respectively [14]. If a magnetic field of magnitude around

$$B^* = \frac{\Delta_{so}}{2\mu_B}\sqrt{1 - \frac{4\Delta_{KK'}^2}{\Delta_{so}(\frac{\mu_{orb}}{\mu_B^2} - 1)}}, \tag{1}$$

is applied along the longitudinal direction of the CNT, the system shown in Fig. 1 can be treated as a spin qubit coupled to a nanomechanical oscillator mode with the following Hamiltonian [9]

$$H = \frac{1}{2}\omega_s\sigma_3 + g(a + a^\dagger)\sigma_1 + \omega_r a^\dagger a, \tag{2}$$

where μ_{orb} and μ_B denote the electronic orbit and spin magnetic moments, Δ_{so} and $\Delta_{KK'}$ are the spin-orbit and intervalley couplings, ω_s is the tunable spin qubit splitting, and ω_r is the frequency of the fundamental bending mode of the CNT described by the annihilation operator a. $\sigma_{1,3}$ are Pauli matrices operating on the two-level spin spaces. Here the spin-phonon coupling

$$g = \Delta_{so}\langle f'\rangle u_0/2\sqrt{2} \tag{3}$$

is independent of the magnetic field B along the CNT, $\langle f'\rangle \equiv \int dz \frac{df(z)}{dz} n(z)$ is the average of the derivative of the waveform $f(z)$ of the phonon mode against the electron density profile $n(z)$ in the QD, and u_0 is the amplitude of the zero-point fluctuations of the phonon mode.

The first flexural eigenmode of the CNT clamped at both sides $z = 0$ and $z = l$ has the form [1]

$$f(z) = \cosh kz - \cos kz + \frac{\cos\beta_0 - \cosh\beta_0}{\sin\beta_0 - \sinh\beta_0}(\sin kz - \sinh kz), \tag{4}$$

where $\beta_0 = 4.730$ and $k = \beta_0/l$. $f(z)$ is normalized to $\int_0^l f^2(x)dx = l$. The confinement potential for the lateral QD embedded in a CNT can be modelled as a parabolic potential [15]

$$V(z) = \frac{1}{2}m^*\omega_0(z - z_c)^2, \tag{5}$$

where m^* is the effective mass of the electron and ω_0 is the characteristic harmonic oscillator frequency, z_c is the center of the parabolic well. Assuming that the electron in the lateral CNT QD is in the ground state, the electron density profile $n(z)$ has the form [16]

$$n(z) = \frac{\alpha}{\sqrt{\pi}}\exp[-\alpha^2(z - z_c)^2], \tag{6}$$

where $\alpha = \sqrt{m^*\omega_0}$.

Because the spin-phonon coupling g is dependent on the electron density profile $n(z)$, we can modulate the spin-phonon coupling strength by altering the electron distribution in the QD. For this reason an electric field E_z is applied along the longitudinal direction of the CNT (Fig. 1 a). Then the total electrostatic potential can be written as

$$V(z) = \frac{1}{2}m^*\omega_0^2(z - z_c)^2 - eE_z(z - z_c) \tag{7}$$

$$= \frac{1}{2}m^*\omega_0^2(z - z_c - \frac{eE_z}{m^*\omega_0^2})^2 - \frac{e^2E_z^2}{2m^*\omega_0^2} \tag{8}$$

Thus this electric field E_z does not modify the energy level spacing of the quantum dot, but does shift the effective center of the quantum dot to $z_c' = z_c + eE_z/(m^*\omega_0^2)$ [17].

As an example we consider the case where the QD is located at the midpoint of the CNT, $z_c = l/2$. With realistic parameters at hand [18, 12], $l = 400$ nm, $u_0 = 2.5$ pm, $\Delta_{so} = 370\mu$eV, $\omega_0/2\pi = 1$ meV,$\alpha = 40/l$, $m^* = \hbar/3R\gamma \simeq 2.2 \times 10^{-31}$kg with the π-band parameter of graphene $\gamma \simeq 533$ MeV nm [16] and the radius of the carbon nanotube $R \simeq 20$ nm, we find the relation between the spin-phonon coupling g and the electric field E_z (Fig.2(b)). The maximum magnitude of $g/2\pi$ is about 0.961 MHz.

Carbon nanotube resonators with high resonance frequencies of several hundred megahertz and a high Q exceeding 10^5 have been reported in [18, 19]. For a resonator of frequency $\omega_r/2\pi = 500$MHz and mechanical quality factor $Q_r = 1 \times 10^5$ we have a resonator damping rate $\gamma_r/2\pi = \omega_r/Q_r = 5 \times 10^4$ Hz$\ll g$. Even in bulk materials such as a one-electron GaAs QD literatures [20, 21] report spin dephasing rate γ_s of several Hz, at the same time near-zero density of state of other phonon modes of a CNT at ω_s can further lower the spin dephasing rate, resulting in a reasonable assumption $\gamma_s \ll g$. Thus the spin-mechanical coupling strength g far exceeds the damping rate γ_r, γ_s, bringing the hybrid system into the so-called "strong coupling" regime.

In the following discussions the resonance condition, $\omega_s = \omega_r$ is assumed.In the interaction picture the Hamiltonian in Eq.(2) can be rewritten into the Jaynes-Cummings form

$$H_{in} = ga\sigma_+ + ga^\dagger\sigma_-, \tag{9}$$

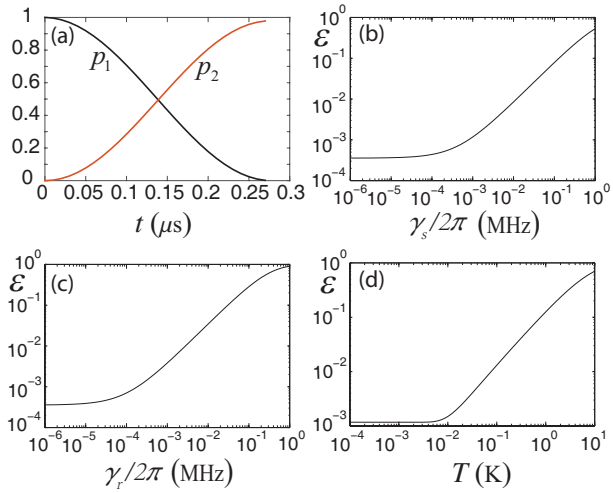

Fig. 3. (color online) (a) The time evolution of the elements of the density operator $p_1(t) = \langle 01|\rho(t)|10\rangle$ and $p_2(t) = \langle 10|\rho(t)|01\rangle$ for initial state $\rho_0 = |10\rangle\langle 01|$. The parameters are $(\omega_r, g, \gamma_r, \gamma_s) = 2\pi \times (500, 0.9, 0.01, 0.01)$MHz and $T = 10$mK. (b) Error ϵ as a function of the spin dephasing rate γ_s for $\gamma_r = 0$ and other unchanging parameters. (c)Error as a function of mechanical decoherence rate γ_r for $\gamma_s = 0$ and other unchanging parameters. (d) Error as a function of the bath temperature T for $\gamma_s = 0$, $\gamma_r = 2\pi \times 0.001$MHz, and other unchanging parameters.

by applying the rotating wave approximation where the counter-rotating terms proportional to $e^{\pm i(\omega_r+\omega_s)t}$ are neglected due to the fact that they oscillate much faster than the terms proportional to $e^{\pm i(\omega_r-\omega_s)t}$, and therefore "average" to zero much faster [22, 23]. Here Pauli matrices $\sigma_+ = |1\rangle\langle 0|$ and $\sigma_- = |0\rangle\langle 1|$ with spin qubit states $|0\rangle$ and $|1\rangle$. Hamiltonian eq6 allows a coherent quantum state transfer between the spin and nanomechanical resonator modes.

3 Numerical simulations of quantum state transfer

To evaluate the system's performance in the anticipated parameter regime, we study the quantum state transfer process of the system with a master equation which includes the unavoidable decoherence. The main source of decoherence is the finite lifetime of the qubit spin and the phonon mode as well as the external phonon bath of nonzero temperature T. The decoherence due to the variation of the electrical field E_z is negligible provided that $\omega_e \ll \omega_s$, where ω_e is the frequency of the field $E_z(t)$ assuming $E_z(t) = E_{z0}\sin(\omega_e t + \phi)$ [17]. Here this condition is well satisfied because ω_e is on the same scale with g (1MHz) and ω_s is on the scale of 100MHz. The master equation for the spin-phonon density operator $\rho(t)$ takes the form

$$\dot{\rho} = -\frac{i}{\hbar}[H_{in}, \rho] + (n_B + 1)\gamma_r D[a]\rho \tag{10}$$

$$+ \quad n_B\gamma_r D[a^\dagger]\rho + \gamma_s D[\sigma_-]\rho, \tag{11}$$

where $n_B = 1/(e^{\omega_r/k_B T} - 1)$ with the Boltzmann constant k_B, and $D[o]\rho = (o\rho o^\dagger - \frac{1}{2}o^\dagger o\rho - \frac{1}{2}\rho o^\dagger o)$.

We analyzed the fidelities of the quantum state transfer operation by numerically solving

Eq.eq7 for initial state $\rho_0 = |10\rangle\langle 01|$, for simplicity, where $|mn\rangle$ denotes the spin and phonon states $|m\rangle$ and $|n\rangle$, respectively. Fig.3(a) shows the evolution of the elements of the density operator $p_1(t) = \langle 01|\rho(t)|10\rangle$ and $p_2(t) = \langle 10|\rho(t)|01\rangle$ when the spin and mechanical qubits are interacting with coupling $g = 2\pi \times 0.9$ MHz of duration time $t = \pi/2g$. To find an estimate for the fidelity of the state transfer operation, we calculate the fidelity $F(\rho_t, \rho) = Tr(\sqrt{\sqrt{\rho}\rho_t\sqrt{\rho}})$ of the desired target state $\rho_t = |01\rangle\langle 10|$ with the actual state ρ that results from the full dynamical evolution. For the experimentally reachable parameters $(\omega_r, g, \gamma_r, \gamma_s) = 2\pi \times (500, 0.9, 0.01, 0.01)$MHz, and $T = 10$mK we have $F(\rho_t, \rho) = 0.979$. Figure 3 (b)-(d) shows the resulting state transfer error $\epsilon = 1 - F$ as a function of the mechanical and spin dissipation rates γ_s and γ_r, and the bath temperature T, respectively.

We now discuss a possible experimental realization of the electric control of the spin-phonon coupling. According to Refs [12, 13] we may fabricate the device on a highly doped silicon wafer terminated with an oxide layer. Gate contacts, source and drain electrodes and catalyst pads are patterned with electron-beam lithography. Finally a nanotube is grown by chemical vapour deposition in a furnace. Applying gate voltage can confine an electron in a quantum dot. A magnetic field is applied along the longitudinal direction of the CNT to generate a spin qubit split. An electrical field is created by applying the voltage across the source and the drain electrodes to modify the spin-phonon coupling strength. The device is placed in a ^{3}He/^{4}He dilution refrigerator at temperature about 10 mK.

4 Conclusion

We have shown how to electrically control the interaction between an electron spin in a lateral CNT QD and a mechanical motion mode of a CNT. The electrical field displaces the electron density distribution, resulting in the change in the strength of the spin-phonon coupling. This electrically controlled spin-phonon coupling can reach the regime of strong interaction. Numerical simulations show that high-fidelity quantum state transfer between spin and phonon qubits is within the reach of the current technology. Potential applications include electrical cooling, state preparation, and readout of a nanomechanical resonator [25, 24, 2], nanomechanical-resonator-mediated quantum interface between optical and spin qubits [3, 26], precision measurement [28, 27], and fundamental tests of quantum theories [29, 30].

Acknowledgments

This work was supported by the National Natural Science Foundation of China (11472247 and 61475168) and by Zhejiang Provincial Natural Science Foundation of China (Grant No. Y6110314).

References

1. M. Poot, and H.S.J. van der Zant (2012), *Mechanical systems in the quantum regime*, Phys. Rep. **511**, pp. 273-335 .
2. P. Rabl,P. Cappellaro, M.V. Gurudev Dutt, L. Jiang, J.R. Maze, and M.D. Lukin (2009), *Strong magnetic coupling between an electronic spin qubit and a mechanical resonator*, Phys. Rev. B **79**, pp. 041302(R).
3. K. Stannigel,P. Rabl, A.S. Sørensen, P. Zoller, and M.D. Lukin (2010), *Optomechanical Transducers for Long-Distance Quantum Communication*, Phys. Rev. Lett. **105**, pp. 220501.
4. B. Simovič, P. Studerus, S. Gustavsson, R. Leturcq, K. Ensslin, R. Schuhmann, J. Forrer, and A.

Schweiger (2006), *Design of QQ-band loop-gap resonators at frequencies of 34–36GHz for single electron spin spectroscopy in semiconductor nanostructures*, Rev. Sci. Instrum. **77**, pp. 064702.
5. F.H.L. Koppens, C. Buizert, K.J. Tielrooij, I.T. Vink, K.C. Nowack, T. Meunier, L.P. Kouwenhoven, and L.M.K. Vandersypen (2006), *Driven coherent oscillations of a single electron spin in a quantum dot*, Nature **442**, pp. 766-771.
6. K.C. Nowack, F.H.L. Koppens, Yu.V. Nazarov, and L.M.K. Vandersypen (2007), *Coherent Control of a Single Electron Spin with Electric Fields*, Science **318**, pp. 1430-1433.
7. G. Salis, Y. Kato, K. Ensslin, D.C. Driscoll, A.C. Gossard, and D.D. Awschalom (2001), *Electrical control of spin coherence in semiconductor nanostructures*, Nature **414**, pp. 619-622.
8. K. Flensberg and C.M. Marcus (2010), *Bends in nanotubes allow electric spin control and coupling*, Phys. Rev. B **81**, pp. 195418.
9. A. Pályi, P.R. Struck, M. Rudner, K. Flensberg, and G. Burkard (2012), *Spin-Orbit-Induced Strong Coupling of a Single Spin to a Nanomechanical Resonator*, Phys. Rev. Lett. **108**, pp. 206811.
10. C. Ohm, C. Stampfer, J. Splettstoesser, and M.R. Wegewijs (2012), *Readout of carbon nanotube vibrations based on spin-phonon coupling*, Appl. Rev. Lett. **100**, pp. 143103.
11. J. Samm, J. Gramich, A. Baumgartner, M. Weiss, and C. Schönenberger (2014), *Optimized fabrication and characterization of carbon nanotube spin valves*, J. Appl. Phys. **115**, pp. 174309.
12. F. Kuemmeth, S. Ilani, D.C. Ralph, and P.L. McEuen (2008), *Coupling of spin and orbital motion of electrons in carbon nanotubes* , Nature (London) **452**, pp. 448-452.
13. T.S. Jespersen, K. Grove-Rasmussen, J. Paaske, K. Muraki, T. Fujisawa, J. Nygård, and K. Flensberg (2011), *Gate-dependent spinorbit coupling in multielectron carbon nanotubes*, Nat. Phys. **7**, pp. 348-353.
14. See Supplemental Material at http://link.aps.org/ supplemental/10.1103/PhysRevLett.108.206811 for more details..
15. S.M. Reimann and M.Manninen (2002), *Electronic structure of quantum dots*, Rev. Mod. Phys. **74**, pp. 1283-1342.
16. A. Secchi and M. Rontani (2013), *Intervalley scattering induced by Coulomb interaction and disorder in carbon-nanotube quantum dots*, Phys. Rev. B **88**, pp. 125403.
17. J.D. Wall (2007), *Parametric spin excitations in lateral quantum dots*, Phys. Rev. B **76**, pp. 195307.
18. G.A. Steele, A.K. Hüttel, B. Witkamp, M. Poot, H. B. Meerwaldt, L.P. Kouwenhoven, and H.S.J. van der Zant (2009), *Strong Coupling Between Single-Electron Tunneling and Nanomechanical Motion*, Science **325**, pp. 1103-1107.
19. A.K. Hüttel, G.A. Steele, B. Witkamp, M. Poot, L.P. Kouwenhoven, H.S.J. van der Zant (2009), *Carbon Nanotubes as Ultrahigh Quality Factor Mechanical Resonators*, Nano Lett. **9**, pp. 2547-2552.
20. S. Amasha, K. MacLean, I. Radu, D.M. Zumbuhl, M.A. Kastner, M.P. Hanson, and A.C. Gossard (2006), *Measurements of the spin relaxation rate at low magnetic fields in a quantum dot*, e-print arXiv:cond-mat/0607110.
21. R. Hanson, L.P. Kouwenhoven, J.R. Petta, S. Tarucha, and L.M.K. Vandersypen (2007), *Spins in few-electron quantum dots*, Rev. Mod. Phys. **79**, pp. 1217-1265.
22. V. Vedral (2005), *Modern Foundations of Quantum Optics*, Imperial College Press (London).
23. E.T. Jaynes and F.W. Cummings (1963), *Comparison of Quantum and Semiclassical Radiation Theories with Application to the Beam Maser*, Proc. IEEE **51**, pp. 89-109.
24. A.D. OConnell, M. Hofheinz, M. Ansmann, R.C. Bialczak, M. Lenander, E. Lucero, M. Neeley, D. Sank, H. Wang, M. Weides, J. Wenner, J.M. Martinis, and A.N. Cleland (2010), *Quantum ground state and single-phonon control of a mechanical resonator*, Nature **464**, pp. 697-703.
25. D. Kleckner and D. Bouwmeester1 (2006), *Sub-kelvin optical cooling of a micromechanical resonator*, Nature (London) **444**, pp. 75-78.
26. W. Yao, R.-B. Liu, and L.J. Sham (2005), *Theory of Control of the Spin-Photon Interface for Quantum Networks*, Phys. Rev. Lett. **95**, pp. 030504.
27. O. Arcizet O, P.F. Cohadon, T. Briant, M. Pinard, and A. Heidmann (2006), *Radiation-pressure cooling and optomechanical instability of a micromirror*, Nature **444**, pp. 71-74.

28. M.D. LaHaye, O. Buu, B. Camarota, and K.C. Schwab (2004), *Approaching the Quantum Limit of a Nanomechanical Resonator*, Science **304**, pp. 74-77.
29. K.C. Schwab and M.L. Roukes (2005), *Putting Mechanics into Quantum Mechanics*, Phys. Today **58**, pp. 36.
30. W. Marshall, C. Simon, R. Penrose, and D. Bouwmeester (2003), *Towards Quantum Superpositions of a Mirror*, Phys. Rev. Lett. **91**, pp. 130401.